Molecular dynamics studies of interaction between hydrogenand carbon nano-carriers

Yun-Che Wang[*], Chun-Yi Wu, Chi Chen and Ding-Shen Yang

Department of Civil Engineering, National Cheng Kung University Tainan 70101, Taiwan

Abstract.   In this work, quantum molecular dynamics simulations (QMD) are preformed to study the hydrogen molecules in three types of carbon nanostructures, C_{60} fullerene, (5,5) and (9,0) carbon nanotubes and graphene layers. Interactions between hydrogen and the nanostructures is of importance to understand hydrogen storage for the development of hydrogen economy. The QMD method overcomes the difficulties with empirical interatomic potentials to model the interaction among hydrogen and carbon atoms in the confined geometry. In QMD, the interatomic forces are calculated by solving the Schrodinger's equation with the density functional theory (DFT) formulation, and the positions of the atomic nucleus are calculated with the Newton's second law in accordance with the Born-Oppenheimer approximation. It is found that the number of hydrogen atoms that is less than 58 can be stored in the C_{60} fullerene. With larger carbon fullerenes, more hydrogen may be stored. For hydrogen molecules passing though the fullerene, a particular orientation is required to obtain least energy barrier. For carbon nanotubes and graphene, adsorption may adhere hydrogen atoms to carbon atoms. In addition, hydrogen molecules can also be stored inside the nanotubes or between the adjacent layers in graphite, multi-layer graphene.

Keywords: quantum molecular dynamics simulation; hydrogen; carbon; fullerene; nanotube; graphene

1. Introduction

The hydrogen storage problem is critical for the development of hydrogen economy (Strobel *et al.* 2006). In fact, the science about hydrogen, even though a very old subject, still requires detailed studies in terms of its behavior under high pressure (Labet *et al.* 2012). In addition to using metal hydrides, or other methods, such as methane carbon dioxide reforming (Ni 2013), nano-cages provide an ideal solution to be a hydrogen carrier. Using carbon carriers for hydrogen storage has been studied by the *ab initio* simulation method (Dodziuki 2005, Ding *et al.* 2007, Pupysheva *et al.* 2008, Lin *et al.* 2008, Singh *et al.* 2009, Kruse *et al.* 2009), as well as experimental methods (Lachawiec *et al.* 2005, Lee and McKee 2008, Stadie *et al.* 2010). In addition to fullerenes, using carbon foam for storing hydrogen by physisorption and chemisorption is reported (Ding *et al.* 2007). For larger nanostructures, or called nanocages, molecules which are formed as a metal organic framework is an plausible candidate (Er *et al.* 2009). To improve the simulation accuracy, efforts have been placed to consider the non-covalent interaction in the hydrogen-carbon system (Kruse *et al.* 2009). By combining experimental and computational

---

∗Corresponding author, Associate Professor, E-mail: yunche@mail.ncku.edu.tw

works, Miller *et al.* (2008) studied the hydrogenation problems on single-wall carbon nanotubes with polyamine reagents. In addition, Wu *et al.* (2010) experimentally demonstrated that through selective hydrogenation the cross-section of carbon nanotubes can be controlled. In addition to using carbon nanotubes for hydrogen storage, significant research has been performed to use the nanotubes as inclusions to enhance physical properties of materials (Li and Sun 2011).

In addition to pure carbon nanostructures, various nanostructures with other chemical elements and structures have been investigated, both computationally and experimentally. From the computational point of view, Averill *et al.* (2009) studied the hydrogenation problem on a single atomic layer of boron nitride and related chemical compound, inspired by the success of single layer graphene. Er *et al.* (2009) investigated the hydrogen storage problem with polylithiated nanostructures. Similar systems have also been probed by Liu *et al.* (2009) for possible enhancement in hydrogen storage in Li-dispersed carbon nanotubes. Wang *et al.* (2009) calculated the problem with hydrogen in Ca-coated fullerenes. In addition, Salam *et al.* (2013) studied the hydrogen adsorption problem on mixed oxides, and Mattesini *et al.* (2006) investigated the mechanical and spectroscopy properties of a metal-organic framework (MOF), which is a potential candidate for high-capacity hydrogen storage. Experimentally, Li and Yang (2006) have demonstrated that hydrogen storage on MOF's can be achieved by the spillover method. In related topics, graphane, a carbohydrate compound that consists hydrogen atoms on single layer, curved or flat, graphene, has been studied with first-principle molecular dynamics (Sofo *et al.* 2007, Tsetseris and Pantelides 2012, Wen *et al.* 2012).

Molecular dynamics (MD) simulation is an important tool to study nanoscale systems that are experimentally inaccessible, and details of the simulation principles and techniques can be found in Tuckerman's book (2010). Recently interactions between aluminum solute atoms and dislocations in magnesium alloys have been studied by the MD simulation (Shen 2013). In addition, the heat resistance of carbon nanoonions have also been studied by the MD method (Wang and Lee 2011). Moreover, Kim *et al.* (2011) have adopted the MD technique to model nanoparticles and polymer, as a part of their multiscale analysis. However, conventional MD simulation relies on empirical interatomic potentials to describe interactions among atoms. The potentials are, in general, fitted with experimental data to determine the necessary parameters in the potential functions. There are two drawbacks in the conventional MD. One is the choice of the potential functional and the other the determined parameters are only valid for bulk materials since they are fitted with experimental data from bulk materials. Use of quantum molecular dynamics (QMD) simulation bypasses the drawbacks since the interatomic force is calculated from the electron interaction, but severely increases computation cost. There are numerous strategies to implement QMD simulation, and in this work the SIESTA code is adopted to simulate hydrogen-carbon systems (Soler *et al.* 2002).

The present studies focus on the interaction between hydrogen and the following three carbon nanostructures: C_{60} carbon fullerene, (5,5) and (9,0) carbon nanotubes and graphene layers. In this work, the carbon nanostructuresare studied with a various number of hydrogen atoms incorporated into the systems to investigate their stability.

2. Quantum molecular dynamics simulation

The general description of the governing equation in quantum molecular dynamics is described in Section 2.1, the density function theory in Section 2.2, and the numerical implementation of the

SIESTA software package in Section 2.3.

2.1 The schrödinger equation

Physical properties of materials at the nano-scales are ultimately determined by their electronic structures and interactions, which are governed by the time-independent Schrödinger equation, as shown in Eqs. (1) and (2). The electron wave function $\Psi = \Psi(x_1, x_2, x_3)$ is governed by the eigenvalue problem with the total energy E as the eigenvalue of the state.

$$H\Psi = E\Psi \tag{1}$$

$$\hat{H} = \sum_i -\frac{1}{2}\nabla_i^2 + \frac{1}{2}\sum_i\sum_I \frac{1}{|r_i - r_j|} + \sum_i\sum_I \frac{-Z_i}{r_i - R_I} \tag{2}$$

The first term is the kinetic operator, involving the Laplacian differential operator, for the number of electrons N. The second term describes the electron-nucleus interactions, the third term for the electron-electron interactions and the last term the nucleus-nucleus interactions. It is noted that the Hamiltonian differential operator H is position-dependent. Position vectors r and R delineate the location of electron and nucleus, respectively. The symbol Z indicates the nucleus charge, and subscripts i and k label the electrons and nuclei, respectively. The number of nucleus is assumed to be M. The Born-Oppenheimer approximation is embedded in the Eq. (1) to simply the many-body Hamiltonian by using the large mismatch between electron and nucleus mass

2.2 Density functional theory

Solving the Schrodinger's equation many-electron systems is not practicable. From the viewpoint of variational calculus, the quantum system must satisfy the following variational condition.

$$\delta\left[\left\langle \Psi \mid \hat{H} \mid \Psi \right\rangle - E\left\langle \Psi \mid \Psi \right\rangle\right] = 0 \tag{3}$$

Here E is the Lagrangian multiplier, and its physical meaning is the total energy of the system, and Hamiltonian operator $\hat{H}$ a partial differential operator, containing kinetic and potential operators. The analytical solution of the above variational problem leads to the following partial differential equation.

$$H\Psi = E\Psi \tag{4}$$

The solution of the above eigenvalue problem yields the energy (E), as the eigenvalue, that is required for ground or excited states, and corresponding wave functions (Ψ). In computation, periodic boundary conditions are adopted for simulate infinite systems, and hence an energy cutoff is introduced for computation efficiency. Mathematically, this cutoff sets how many terms would be included in the fourier series, i.e., superposition of plane waves.

2.3 SIESTA software package

The exact solution of the Schrödinger equation for the many-body problem are unattainable,

and hence the density functional theory (DFT) is introduced to solve the Schrödinger equation as a variational problem numerically. In this work, the software package SIESTA (Spanish Initiative for Electronic Simulations with Thousands of Atoms) is adopted to calculate the hydrogen-carbon systems (Soler *et al.* 2002). The positions of the hydrogen atoms are first manually placed inside the carbon nanocages. The conjugate gradient (CG) method is not adopted in this study. All energy minimization is done by prolong QMD simulations in the time domain.

The SIESTA program uses the self-consistent algorithm to solve the one-particle Kohn-Sham (KS) Schrodinger-like equation, and finds the eigenvectors (wave function) and eigenvalues (energy) of the systems. The solution technique is based on the expansion of wave functions using localized, numerical orbitals as basis sets. In this work, the diagonal method for the numerical scheme in SIESTA was adopted. The solution technique is based on the expansion of wave functions using localized, numerical orbitals as basis sets of finite range. Furthermore, norm-conserving Troullier-Martines pseudo potentials in the Kleinman-Bylander factorized form and a double - ζ basis set. The generalized gradient approximation for the exchange-correlation potential was implemented.

3. Results and discussion

In this section, the hydrogen and fullerene system is reported first. Then, the hydrogen and carbon nanotube system is discussed in Section 3.2. Finally, the interaction between hydrogen and graphene is discussed in Section 3.3.

3.1 The hydrogen and C_{60} fullerene system

It is well known that C_{60} fullerene is one of the most stable chemical compounds. By introducing hydrogen into the fullerene, denoted as the $H_n@C_{60}$ chemical compound, one may utilize the fullerene as a hydrogen carrier. However, to the present day, a methodology to put hydrogen inside the fullerene by physical means, i.e., through pressure and temperature, is still lacking. More discussions can be found later in the text before the Conclusion section. Fig. 1(a) shows the six hydrogen atoms (i.e., $H_6@C_{60}$) form 3 H_2 hydrogen molecules by the quantum molecular dynamics, after equilibration. However, it isnoted that with large amount of hydrogen atoms inside the fullerene, it is likely to form bonding between the hydrogen and carbon atoms. In addition, the pressure inside the fullerene drastically increases with the number of hydrogen atoms, as discussed in Pupysheva *et al.* (2009). With this large increase in pressure, the work by Labet *et al.* (2012) is crucial to understand the nature of hydrogen bond under high pressure. Through our quantum molecular dynamics simulations, Fig. 1(b) shows the formation energy, E_f, as calculated by Eq. (8) below, increases with the number of hydrogen atoms, as well as the volume of the fullerene.

$$E_f = E(H_n@C_{60}) - E(C_{60}) - \frac{n}{2}E(H_2) \qquad (5)$$

The formation energy calculated in this work is consistent with that reported by Pupysheva *et al.* (2008), but slightly larger due to differential initial arrangements of the hydrogen atoms. Both of our models show the breakage of the fullerene with 58 hydrogen atoms inside. In our models, hydrogen atoms are initially put in the fullerene in pairs as hydrogen molecules. The distances
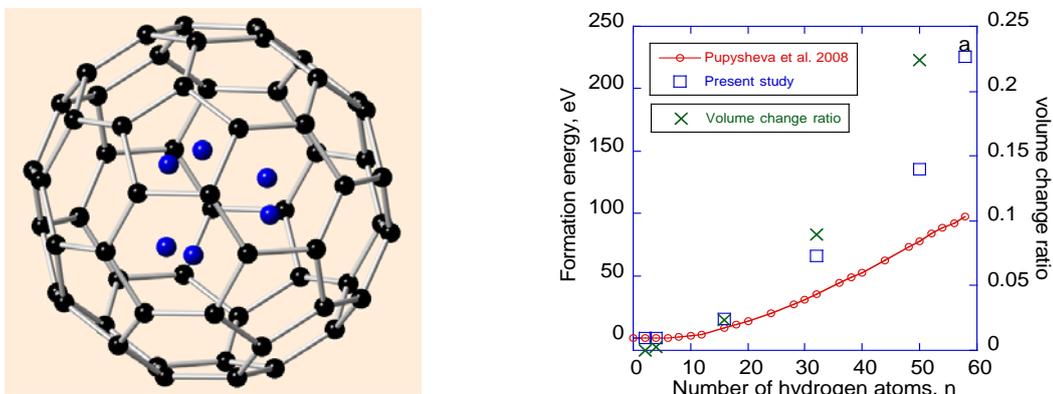
Fig. 1 (a) The $H_6@C_{60}$ molecular dynamics model, and (b) formation energy and volume change ratio versus the number of hydrogen atoms.
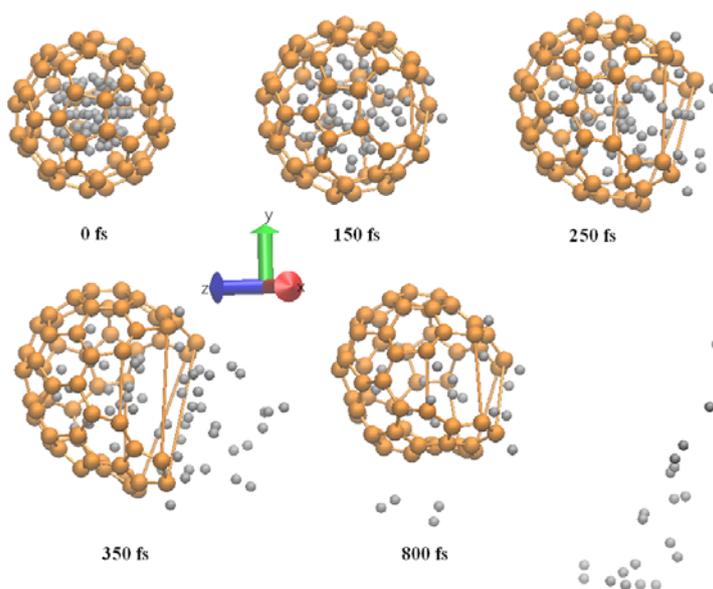

Fig. 2 Time evolution of the $H_{58}@C_{60}$ model to show the breakage of the fullerene cage

between hydrogen molecules were checked large enough to avoid strong interatomic repulsion. Then, significantly long-time QMD simulations were conducted to reach MD equilibrium. Slightly changing the initial configuration would not change the final configuration. We acknowledge that our models may not be as ideal as those reported in the literature after significantly structural optimization through the conjugate gradient method to reach a lowest energy state. Hence, they show slightly larger formation energy, which may include energy associated with hydrogen under confined geometry (Labet *et al.* 2012) and interaction between carbon and hydrogen. Nonetheless, the literature model represents one physical realization of the system, and our model represents another physically acceptable realization of the hydrogen atoms inside the fullerene. Without using

the optimal structure, our work here can be considered as a study of perturbed systems, which show slightly larger energy. The label 'a' on Fig. 1(b) indicates that for $n = 58$ the formation energy is calculated after the fullerene is broken and reaches MD equilibrium. In addition, Volume change of the C_{60} fullerene encapsulated with hydrogen atoms indicates the bulk elastic behavior of the nanostructure under internal pressure.

Fig. 2 shows the breakage of the fullerene with $n = 58$ due to exceptional large pressure generated by the hydrogen. At 150 femto seconds (f_s), some of the hydrogen escapes from the fullerene, and then at 250 f_s the C_{60} opens with large amount of hydrogen moving outwards. Between 350 and 800 f_s it can be seen that the fullerene becomes smaller, and appears to recover its original shape, except for the damaged region. The unrealistically longer carbon-carbon bonds, as shown in yellow color, indicate the original connection between the two carbon atoms. It is observed that hydrogen atoms that escape from the cage form hydrogen molecules. Furthermore, many hydrogen atoms are attached to carbon atoms that are around the damaged area to form *C-H* bonds.

Under the thin-wall assumption, the internal pressure p would contribute the stresses in the fullerene as

$$\sigma_{rr} = -p + 7P(1 + \frac{h}{a})^3 \tag{6}$$

$$\sigma_{\varphi\varphi} = \sigma_{\varphi\varphi} = \frac{p}{4} + \frac{5P}{4}\left(1 + \frac{h}{a}\right)^3 \tag{7}$$

where h is the wall thickness and a the inner radius of the fullerene. The subscripts follow the standard usage in the continuum mechanics. To the first order approximation, the stress in the wall of the fullerene is on the same order of the internal pressure. By using the expression established by Pupysheva *et al.* (2008), the internal pressure $p = 2C\varepsilon_{rr}/R$ and the strained radius can be calculated from un-strained radius by $R = R_0(1 + \varepsilon_{rr})$, where $R_0 = 0.356$ nm. When $n = 50$, the radial strain of the fullerene is about 7%, as can be inferred from Fig. 1(b). Under this deformation, the in-plane stiffness of the fullerene is about 300 N/m, as reported in Pupysheva *et al.* (2008). Hence, the internal pressure is estimated to be about $p = 110$ GPa. Under such a high stress, reaction rates, estimated from the transition state theory, may be largely increased, hence the characteristic bond-cleavage time, i.e. the inverse of the reaction rate, can be significantly reduced (Drexler 1992). For the C-C bond at 300 K, Drexler (1992) estimated that cleavage time may be reduced by a factor of 1000 when the atomic force in a C-C bond increases 1 nN. From the MM2 bond stretching potential, a 0.07 bond strain would require 3.2 nN for the C-C bond as a rough estimation (Drexler 1992, pp. 44-45). Hence, our observed such a short cleavage time can be qualitatively explained by the transition state theory with the consideration of mechanical loading. However, quantitative calculations require further studies in the future. As shown in Fig. 2, the beginning of the cage opening is about at time equal to 150 f_s, and a noticeable cage opening occurs at time 250 f_s. This finding is consistent with data reported by Pupysheva *et al.* (2008) in terms of orders of magnitude, even though carbon-carbon bond cleavage time usually occur in the picosecond range from chemical reactions (Bockman *et al.* 1996, Holbrook *et al.* 1996). In addition, in reality, it is unlikely that one can pack 58 atoms in the C_{60} fullerene, and hence the breakage reflects the instability of the hydrogen-fullerene system due to excessive deformation that cannot be stored in the fullerene.
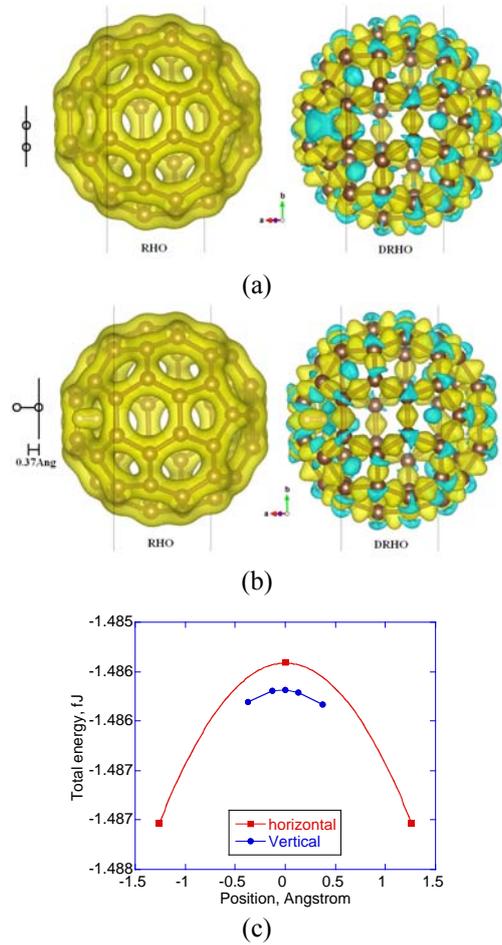
(a)

(b)

(c)

Fig. 3 (a) The horizontal configuration of the hydrogen molecule being placed on the wall of the fullerene, (b) the vertical configuration of the hydrogen molecule being placed in touch of the wall of the fullerene, and (c) the ground-state energy of the hydrogen-fullerene system versus various locations of the hydrogen molecule.

In order to test the energy penalty for a hydrogen molecule passing through the fullerene from outside to inside without breaking the C_{60}, Figs. 3(a) and 3(b) show the two arrangements of thehydrogen molecule, called he horizontal and vertical, respectively. The color in (a) and (b) indicate the valence pseudocharge density ρ, and the difference between valence pseudocharge density and sum of atomic valence pseudocharge density δ_ρ, defined by

$$\delta\rho(r) = \rho(r) - \rho_a(r) \tag{8}$$

The pseudocharge density describe the electronic structures of the atoms in the system. As can be seen in Fig. 3(c), the energy barrier for the horizontal case is much larger than that of the vertical case. Therefore, without breaking the fullerene, we propose that the refilling and release mechanism of hydrogen in fullerene should involve the orientation of the hydrogen molecules to reach a position with least energy barrier. The results of Fig. 3 were obtained by manually place
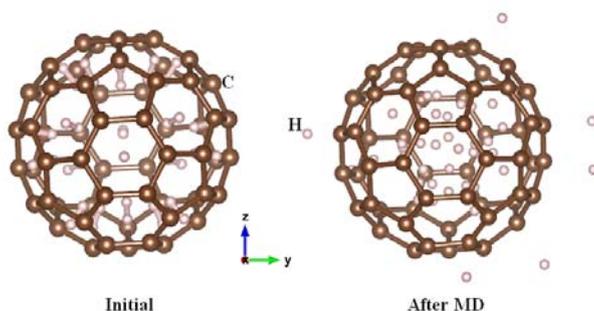
Fig. 4 The initial (one of the atoms for a H_2 molecule is on the surface of the fullerene) and final (after about 110 f_s) configuration of the hydrogen-fullerene system. Energy equilibrium was obtained for the simulation time

the hydrogen molecules in the desired position around the fullerene, and then calculated with equilibration quantum molecular dynamics simulation.

To further test the vertical arrangements of hydrogen molecules on the fullerene, we placed hydrogen molecules on all the hexagonal ring on the fullerene, and perform QMD simulation on the system. One of the two atoms of the hydrogen molecule was placed on the surface of the fullerene. Results are shown in Fig. 4. After about 110 f_s the system reaches equilibration in terms of energy, most of the hydrogen atoms were trapped inside the fullerene and some of them escaped away. Such as fast reaction cannot be explained by classical transition state theory, since the arrangement of the initial atomic configuration is artificially at an extremely high energy state. After a relatively short amount of time, the hydrogen bond of hydrogen molecules would be severed by the energy field of the fullerene. It is found that a large amount of hydrogen atoms inside the fullerene form the hydrogen molecules. Furthermore, some hydrogen atoms may also be attached to the carbon atoms to form C-H bond. For the hydrogen atoms being left outside of the fullerene, after a sufficient amount of time, they may form hydrogen molecules. In addition, these results are very sensitive to the initial positions of the hydrogen molecules. If the initial vertical insertion of the hydrogen molecules into the fullerene is not deep enough, less hydrogen atoms would be found in the fullerene.

3.2 The hydrogen and (5,5) or (9,0) carbon nanotube system

Carbon nanotubes have long to thought to be used as a hydrogen storage device. Figs. 5(a) and 5(b) show the physisorption of hydrogen atoms on the outside of the (5,5) carbon nanotubes for one and seven hydrogen atoms, respectively. It can be seen that for one hydrogen atom, the physisorption is strong enough to deform the carbon nanotube.It is expected to observe that more hydrogen atoms being adsorbed on the outside of the nanotubes. However, as shown in Fig. 5(b), it is possible for the hydrogen to form H_2 molecules, and escape from the weak field generated by physisorption between the hydrogen and carbon atoms. The rational for this particular case is the initial configuration to associate two hydrogen atoms with a carbon ring, hence the competition between the two hydrogen atoms to fight for a carbon ring causes both of the hydrogen atoms cannot be physically absorbed onto the ring, and form a neutral hydrogen molecule. Once the hydrogen molecule is formed, the interaction between the molecule and nanotubes relies on the
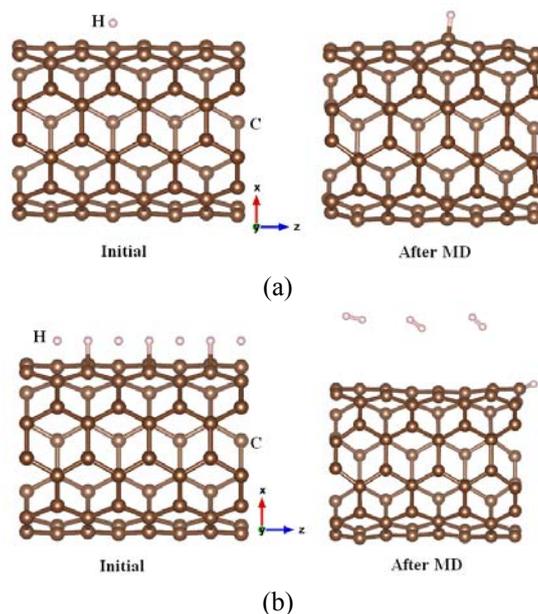
Fig. 5 (a) An hydrogen atom physically adsorbed on the outside of the (5,5) carbon nanotube for initial and after 160 f_s, and (b) interaction between seven hydrogen atoms and the (5,5) nanotubes for initial and after 45 f_s. Energy equilibrium was obtained for the two simulation times
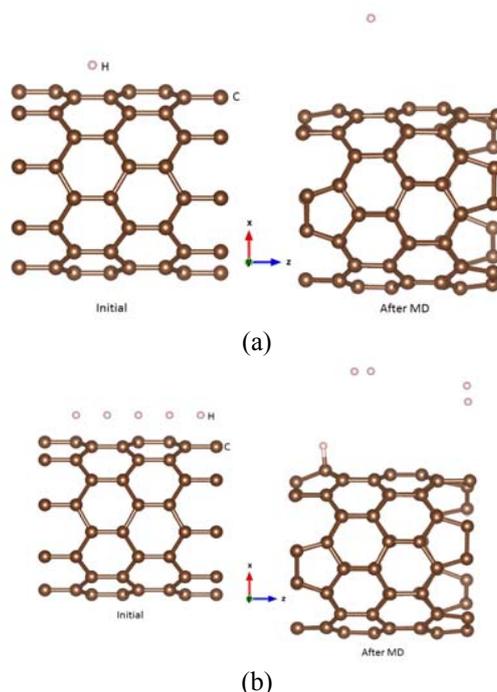

Fig. 6 For the zigzag (9,0) carbon nanotube, (a) an hydrogen atom cannot be physically adsorbed on its outer surface, and (b) interaction between six hydrogen atoms and the nanotube. The label "After MD" indicates an QMD run for 78 f_s, and energy equilibrium was obtained

van der Waal type weak force. Therefore, the hydrogen molecule may not stay near the nanotube. Fig. 6 shows the results of a similar study on the zigzag (9,0) carbon nanotube. In Fig. 6(a), a single hydrogen atom near the tube cannot be adsorbed by the tube due to longer distance between hydrogen and carbon, as well as the curvature effects. For multiple hydrogen atoms, as shown in Fig. 6(b), one of the hydrogen was able to be adsorbed on the tube. By comparing Figs. 5 and 6, it is seen that the chirality for the armchair and zigzag nanotube does not significantly change the adsorption behavior. Both of them can adsorb hydrogen, and from the kinetics viewpoint, the docking sites need to be carefully chosen to make a successfully adsorption. Fully hydrogenated optimal carbon nanotubes may be affected by the chirality, and require further studies.

It is remarked that the local curvature of the nanotube introduces a fractional sp^3-hybridized bond character on the top of the dominate sp^2-hybridized bond, which makes the nanotubes behave differently from graphene, as discussed in the next section. Smaller tubes have stronger sp^3-hybridized characteristics, and hence more deviations from graphene.In addition to physisorption, there are different ways to utilize nanotubes to store hydrogen. For example, one can use the nanotubes similar to the fullerene, and store the hydrogen inside the tubes, which require further studies to show its performance as a hydrogen carrier.

3.3 The hydrogen and graphene system

To test the fully hydrogenation on the single-layer graphene, Fig. 6 shows that, after equilibration simulation with the NVT at 300 K, six out of 24 hydrogen atoms remain physically adsorbed, and chemically adsorbed, on the graphene. Other hydrogen atoms move away from graphene, and some of them form hydrogen molecule. Furthermore, after equilibration, the graphene may no longer stay in a plane, and become H-induced corrugated configuration, as seen in the bottom figure in Fig. 7.

Fig. 8 shows the formation energy per atom of the hydrogen-graphene system, also known as graphane (Sofo *et al.* 2007, Tsetseris and Pantelides 2012, Wen *et al.* 2012), versus number of hydrogen atoms on the graphene. The formation energy is defined as total system energy, subtracted from graphene-only energy and escaped-hydrogen-molecule energy, in a manner similar to Eq. (5). Energy normalization is done by dividing formation energy to total number of atoms without counting escaped hydrogen atoms. In most literature papers about graphane, they focus on fully hydrogenated graphane, for its formation and stability problems. Here, we focus on the kinetics by monitoring the hydrogen behavior on the graphene, as shown in Fig. 7. For the data points, labeled as 'a', 'b' and 'c', they are calculated from the system shown in Fig. 7, containing 32 carbon atoms in a unit cell (referred to the small unit cell case). For 'a', one hydrogen atom is on the graphene, and after equilibration, no hydrogen atoms escaped. For 'b' and 'c', respectively, 12 and 32 hydrogen atoms initially were put in the system, and after equilibration, 4 and 6 H atoms remain on the graphene, meaning 8 and 26 hydrogen atoms escaped. The slopes of the energy versus number of hydrogen atoms are calculated. The data point 'd' was obtained from a different model that contains160 C in the graphene and 24 H atoms (initially) in a unit cell (referred to the large unit cell case), and after MD equilibrium 18 hydrogen atoms remain on the graphene.The atomic percentages of hydrogen for the '*a*', '*b*', '*c*' and '*d*' are 0.031, 0.125, 0.1875 and 0.1125, respectively.

The negative energy indicates the formation of such hydrocarbon compounds requires energy less than graphene. It can be seen that larger hydrogen atoms reduce formation energy per atom in a linear fashion. From the small unit cell case (32 carbon atoms), the slope of the formation
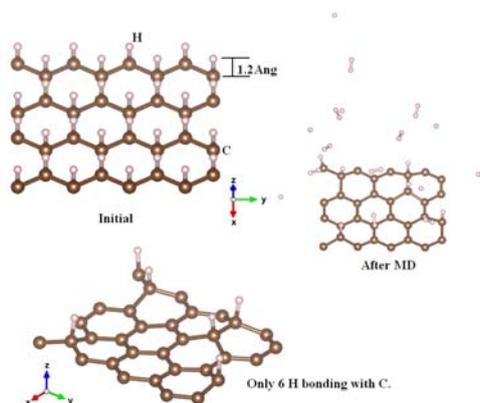
Fig. 7 Comparison of formation energy for various number of hydrogen atoms in the C60 fullerene. Only six hydrogen atoms bonded with the graphene by physisorption. The label "After MD" indicates an QMD run for 400 f_s, and energy equilibrium was obtained
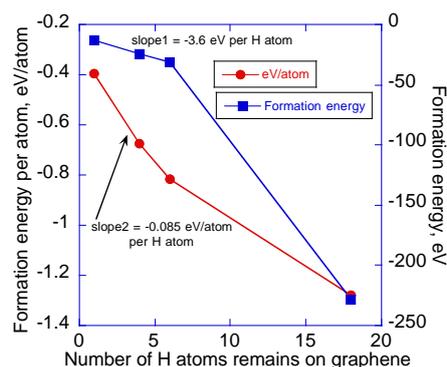

Fig. 8 Formation energy of the hydrogen-graphene system. Normalization was with respect to the total number of atoms in the model, without counting escaped hydrogen molecules

energy, 'slope1', is -3.6 eV when adding one more hydrogen atom on the graphene. Further, the slope of the formation energy per atom in the system, 'slope2', is -0.085 eV/atom when one more hydrogen atom is adsorbed on the graphene. Sofo *et al.* (2007) reported formation energy per atom to be -0.15 eV/atom for fully hydrogenated chair-type graphane and -0.1 eV/atom for fully hydrogenated boat-type graphane at 0.5 atomic percent hydrogen. It is noted that since our system is not fully hydrogenated ones, nor a perfect chair-type or boat-type, our data are not to be quantitatively compared with literature data. However, qualitatively, our data are consistent with the literature data. In our simulation methodology, for the small unit cell (32 carbon atoms) case, hydrogen atoms near the center of the graphene escape more. For the large unit cell case (160 carbon atoms), hydrogen atoms near the edge of the graphene escape more.

It is known that spillover or other mechanism is required to separate the hydrogen molecule into two hydrogen atoms for them being physically adsorbed on graphene, as discussed in Fig. 7. However, without catalyst effects on hydrogen separation, it is entirely possible for hydrogen molecules being stored in multilayered graphene. Fig. 9 demonstrates this idea by using the

three-layer graphenewith six hydrogen molecules initially placed between the layers. In Fig. 9(a) the simulation temperature was 300 K, and in (b) the temperature was 500 K. Both of the top view and side view are plotted.It can be seen that, regardless of temperature, the hydrogen molecules remain as the H_2 form, and are trapped in the graphene layers.

Fig. 10 shows the hydrogen atoms being adsorbed inside the three-layer graphite at 300 K. In the initial structure, single hydrogen atoms were placed separately in the middle of the graphitic layers. After MD equilibrium, most hydrogen atoms were adsorbed on the middle layer. Therefore, both molecular or atomic forms of hydrogen may be stored in graphite. This results may shed light on using graphite to store hydrogen molecules, instead of the atomic form of hydrogen through physisorption or chemisorption. Refilling and extraction mechanisms of hydrogen into and out of the graphite require further computational and experimental studies.
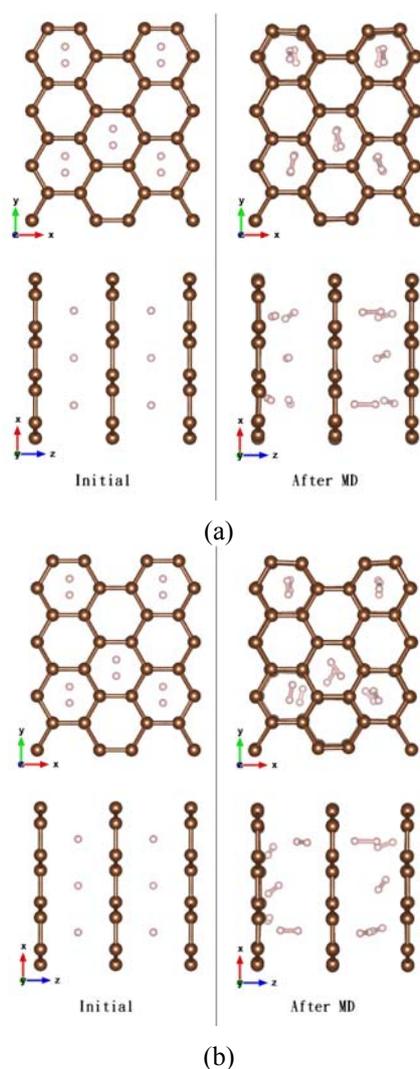

(a)

(b)

Fig. 9 Hydrogen molecules in the three-layer graphene at (a) 300 K and (b) 500 K. The label "After MD" indicates an QMD run for 35 f_s, and energy equilibrium was obtained
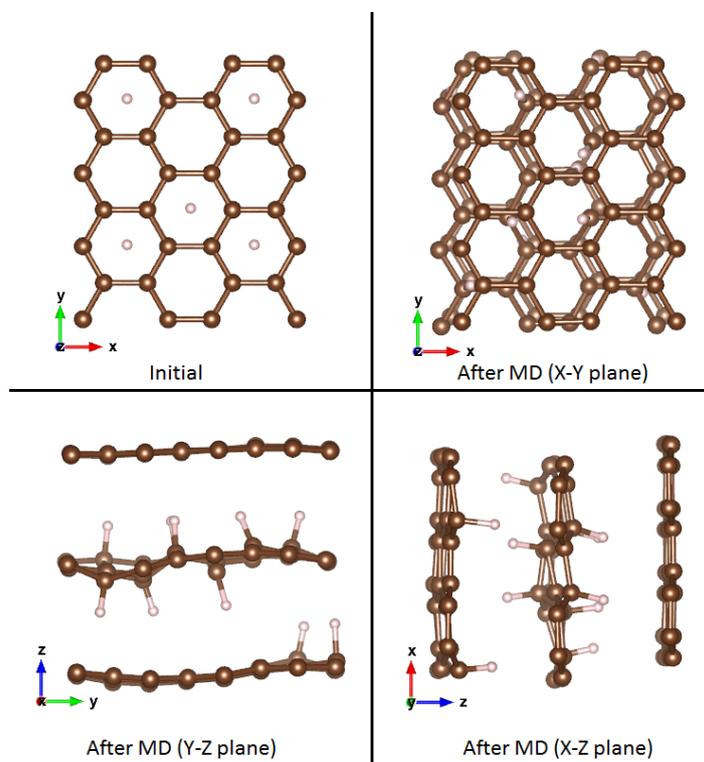
Fig. 10 Hydrogen atoms being adsorbed in the three-layer graphene at 300 K. The label "After MD" indicates an QMD run for 400 *fs*, and energy equilibrium was obtained

For the cases studied in Figs. 5, 6, 7, 9 and 10, the initial distribution of the hydrogen atoms is not sensitive to the final results. All simulations were done at 300 K with the QMD methodology, except for Fig. 9(b), which was simulated at 500 K. From the case in Fig. 9(b), it can be seen that at the elevated temperature the hydrogen molecules can still be trapped in the layers. However, in general, higher temperature provides more thermal energy to the motion of nuclei, hence the trajectories of the atoms may be significantly changed, and this requires further research work in the future.

Through our studies here it is realized that by any physical means, by changing pressure or temperature, it is difficult to insert hydrogen molecules into a fullerene, even though it is attractive to be used as a hydrogen carrier with a large hydrogen-carbon ratio. Without a mechanism to construct fullerenes with encapsulated hydrogen, using fullerenes for such as a purpose may not be advised. However, it is widely accepted that the outer surface of the fullerene may be doped to carry hydrogen (Dresselhaus *et al.* 1996), by a mechanism similar to that for carbon nanotube or graphene. It is emphasized that our investigationshere do not start fromoptimal structures for equilibrium studies, but focus on kinetics, i.e., from one state to another, in order to verify stability of the systems. Hence, in Figs. 3 and 4, attempts have been made to study the behavior of hydrogen moving into the fullerene in terms of charge densities and MD stable configurations. Challenges to overcome energy barrier on the wall of the fullerene to resist the insertion of the hydrogen require further studies in the future. Along a different line of research, it may be possible

to construct the hydrogen-fullerene system by chemical synthesis. The challenges may also apply to graphite, because it requires a mechanism to put hydrogen atoms in between the layers. Hence, the most promising carbon carriers for hydrogen are graphene (or graphane) and the outer surface of the nanotubes (or graphane nanotubes). However, it seems plausible to insert hydrogen into un-capped nanotubes. In addition, defected carbon nanotubes may have better performance in terms of carrying hydrogen due to its active carbon around defects.

4. Conclusions

In this work, the interactions between hydrogen and the C_{60} fullerene, (5,5) and (9,0) carbon nanotubes, as well as single-layer and multi-layer graphene, have been studied with the quantum molecular dynamics simulation. Significant amount of the hydrogen may be stored in fullerene, depending on the size. Inside the fullerene, the bonding nature of the hydrogen is complex due to high pressure for large n. For small n, the hydrogen atoms may form hydrogen molecules or single atomic form being adsorbed to a carbon atom. However, with pressure built up in the fullerene for a large amount of hydrogen, breakage of the fullerene is inevitable. For hydrogen molecules passing though the fullerene, a particular orientation is required to obtain least energy barrier. Carbon nanotubes may also physically adsorb the hydrogen atoms on the surface, or store them inside the tubes. From the hydrogen-graphene systems, adsorption of hydrogen on carbon atoms can be achieved. Once hydrogen is adsorbed, the graphene cannot maintain its two-dimensional feature, but is slightly deformed out-of-plane. In addition, the hydrogen molecules may be stored in multi-layer graphene, but mechanisms to put in and pull out hydrogen in the layers require further studies.

Acknowledgements

References

Averill, F.W., Morris, J.R. and Cooper, V.R. (2009), "Calculated properties of fully hydrogenated single layers of BN, BC2N, and graphene: graphene and its BN-containing analogues", *Phys. Rev. B*, **80**, 195411.

Bockman, T.M., Hubig, S.M. and Kochi, J.K. (1996), "Direct observation of carbon-carbon bond cleavage in ultrafast decarboxylations", *J. Am. Chem. Soc.*, **119**, 4502-4503.

Ding, F., Lin, Y., Krasnov, P.O. and Yakobson, B.I. (2007), "Nanotube-derived carbon foam for hydrogen sorption", *J. Chem. Phys.*, **127**, 164703.

Dodziuki, H. (2005), "Modeling complexes of H2 molecules in fullerenes", *Chem. Phys. Lett.*, **410**, 39-41.

Dresselhaus, M.S., Dresselhaus, G. and Eklund, P.C. (1996), *Science of Fullerenes and Carbon Nanotubes*, Academic Press, San Diego, CA, USA.

Drexler, K.E. (1992), *Nanosystems – Molecular Machinery*, Manufacturing and Computation, John Wiley & Sons, New York, USA.

Er, S., Wijs de, G.A. and Brocks, G. (2009), "Hydrogen storage by polylithiated molecules and

nanostructures", *J. Phys. Chem. C*, **113**(20), 8997-9002.

Holbrook, K.A., Pilling, M.J. and Robertson, S.H. (1996), *Unimolecular Reactions*, John Wiley & Sons, New York, USA.

Kim, B.R., Pyo, S.H., Lemaire, G. and Lee, H.K. (2011), "Multiscale approach to predict the effective elastic behavior of nanoparticle-reinforced polymer composites", *Interact. Multiscale Mech.*, **4**, 173-185.

Kruse, H. and Grimme, S. (2009), "Accurate Quantum Chemical Description of Non-Covalent Interactions in Hydrogen Filled Endohedral Fullerene Complexes", *J. Phys. Chem.C*, **113**, 17006-17010.

Labet, V., Gonzalez-Morelos, P., Hoffmann, R. and Ashcroft, N.W. (2012), "A fresh look at dense hydrogen under pressure. I. An introduction to the problem, and an index probing equalization of H-H distances", *J. Chem. Phys.*, **136**, 074501.

Lachawiec, A.J., Qi, G. and Yang, R.T. (2005), "Hydrogen storage in nanostructured carbons by spillover: bridge-building enhancement", *Langmuir*, **21**, 11418-11424.

Lee, T.B. and McKee, M.L. (2008), "Endohedral hydrogen exchange reactions in C60 (nH2@C60, n=1-5): comparison of recent methods in a high-pressure cooker", *J. Am. Chem. Soc.*, **130**, 17610-17619.

Li, R. and Sun, L.Z. (2011), "Dynamic mechanical analysis of silicone rubber reinforced with multi-walled carbon nanotubes", *Interact. Multiscale Mech.*, **4**, 239-245.

Li, Y. and Yang, R.T. (2006), "Significantly enhanced hydrogen storage in metal-organic frameworks via spillover", *J. Am. Chem. Soc. JACS Commun.*, **128**, 726-725.

Lin, Y., Ding, F. and Yakobson, B.I. (2008), "Hydrogen storage by spillover on graphene as a phase nucleation process", *Phys. Rev. B*, **78**, 041402.

Liu, W., Zhao, Y.H., Li, Y., Jiang, Q. and Lavernia, E.J. (2009), "Enhanced hydrogen storage on Li-dispersed carbon nanotubes", *J. Phys. Chem. C*, **113**, 2028-2033.

Mattesini, M., Soler, J.M. and Yndurain, F. (2006), "Ab initio study of metal-organic framework-5 $Zn_4O(1,4\text{-benzenedicarboxylate})_3$: an assessment of mechanical and spectroscopic properties", *Phys. Rev. B*, **73**, 094111.

Miller, G.P., Kintigh, J., Kim, E., Weck, P.F., Berber, S. and Tomanek, D. (2008), "Hydrogenation of single-wall carbon nanotubes using polyamine reagents: combined experimental and theoretical study", *J. Am. Chem. Soc.*, **130**, 2296-2303.

Ni, M. (2013), "Methane carbon dioxide reforming for hydrogen production in a compact reformer – a modeling study", *Adv. Energy Res.*, **1**, 53-78.

Pupysheva, O.V., Farajian, A.A. and Yakobson, B.I. (2008), "Fullerene Nanocage Capacity for Hydrogen Storage", *Nano Lett.*, **8**, 767-774.

Salam, M.A., Sufian, S. and Lwin, Y. (2013), "Hydrogen adsorption study on mixed oxides using the density functional theory", *J. Phys. Chem. Solids*, **74**, 558-564.

Shen, L. (2013), "Molecular dynamics study of Al solute-dislocation interactions in Mg alloys", *Interact. Multiscale Mech.*, **6**, 127-136.

Singh, A.K., Ribas, M.A. and Yakobson, B.I. (2009), "H-spillover through the catalyst saturation: an ab initio thermodynamics study", *ACS Nano*, **3**, 1657-1662.

Sofo, J.O., Chaudhari, A.S. and Barber, G.D. (2007), "Graphane: a two-dimensional hydrocarbon", *Phys. Rev. B*, **75**, 153401.

Soler, J.M., Artacho, E., Gale, J.D., Garcia, A., Junquera, J., Ordejon, P. and Sanchez-Portal, D. (2002), "The SIESTA method for ab initio order-N materials simulation", *J. Phys. Cond. Mat.*, **14**, 2745-2779.

Stadie, N.P., Purewal, J.J., Ahn, C.C. and Fultz, B. (2010), "Measurements of hydrogen spillover in platinum doped superactived carbon", *Langmuir*, **26**, 15481-15485.

Strobel, R., Garche, J., Moseley, P.T., Jorissen, L. and Wolf, G. (2006), "Hydrogen storage by carbon materials", *J. Power Sources*, **159**(2), 781-801.

Tsetseris, L. and Pantelides, S.T. (2012), "Hydrogen uptake by graphene and nucleation of graphane", *J. Mater. Sci.*, **47**(21), 7571-7579.

Tukerman, M.E. (2010), *Statistical Mechanics: Theory and Molecular Simulation*, Oxford University Press, Oxford, UK.

Wang, Q., Sun, Q., Jena, P. and Kawazoe, Y. (2009), "Theoretical study of hydrogen storage in Ca-coated

fullerenes", *J. Chem. Theory Comput.*, **5**, 374-379.

Wang, X. and Lee, J.D. (2011), "Heat resistance of carbon nanoonions by molecular dynamics simulation", *Interact. Multiscale Mech.*, **4**, 247-255.

Wen, X.D., Yang, T., Hoffmann, R., Ashcroft, N.W., Martin, R.L., Rudin, S.P. and Zhu, J.X. (2012), "Graphane nanotubes", *ACS Nanos*, **6**, 7142-7150.

Wu, G., Wang, J., Zeng, X.C., Hu, H. and Ding, F. (2010), "Controlling cross section of carbon nanotubes via selective hydrogenation", *J. Phys. Chem. C.*, **114**, 11753-11757.